Size-Restricted Proton Transfer within Toluene-Methanol Cluster Ions

Chi-Tung Chiang,[†] Kevin S. Shores,[†] Marek Freindorf,[‡] Thomas Furlani,[‡] Robert L. DeLeon,[†] and James F. Garvey*,[†]

*Department of Chemistry, University at Buffalo, State University of New York at Buffalo,
Buffalo, New York 14260-3000 and Center for Computational Research, University at Buffalo,
State University of New York at Buffalo, Buffalo, New York*

Received: May 9, 2008; Revised Manuscript Received: September 9, 2008

To understand the interaction between toluene and methanol, the chemical reactivity of $\{(C_6H_5CH_3)(CH_3OH)_{n=1-7}\}^+$ cluster ions has been investigated via tandem quadrupole mass spectrometry and through calculations. Collision Induced Dissociation (CID) experiments show that the dissociated intracluster proton transfer reaction from the toluene cation to methanol clusters, forming protonated methanol clusters, only occurs for $n = 2-4$. For $n = 5-7$, CID spectra reveal that these larger clusters have to sequentially lose methanol monomers until they reach $n = 4$ to initiate the deprotonation of the toluene cation. Metastable decay data indicate that for $n = 3$ and $n = 4$ $(CH_3OH)_3H^+$ is the preferred fragment ion. The calculational results reveal that both the gross proton affinity of the methanol subcluster and the structure of the cluster itself play an important role in driving this proton transfer reaction. When $n = 3$, the cooperative effect of the methanols in the subcluster provides the most important contribution to allow the intracluster proton transfer reaction to occur with little or no energy barrier. As $n \geq 4$, the methanol subcluster is able to form ring structures to stabilize the cluster structures so that direct proton transfer is not a favored process. The preferred reaction product, the $(CH_3OH)_3H^+$ cluster ion, indicates that this size-restricted reaction is driven by both the proton affinity and the enhanced stability of the resulting product.

I. Introduction

The structure of gas-phase clusters has become a subject of great interest and has been studied extensively using supersonic molecular beam techniques supported by spectroscopic detection.[1−8] In such a unique finite cluster environment, intermolecular forces can be investigated as a function of solvation. The goal is to understand the microscopic details of many chemical, physical, and biological phenomena in bulk solution phase or in the upper atmosphere, such as proton transfer reactions, electron transfer reactions, particulate formation, and aerosol formation. In particular, intracluster reactions can be activated by microsolvation since quite often a reaction requires a minimum number of solvent molecules to reduce the activation barrier. In the most extreme cases, a single, solvent molecule can serve as a catalyst that sufficiently lowers the activation barrier and allows a reaction to occur that would not be observed otherwise.[1] The importance of solvation is determined substantially by the chemical properties of the solute and solvent molecules.[4−14]

An aromatic cation can be considered to be a relatively strong acid since the corresponding base is a stable neutral radical.[15,16] In the case of clusters of a benzene cation solvated by water molecules, this prototype system has been studied extensively both by employing various mass spectrometric methods and theoretical calculations.[8−11] Both experimental data and calculational results support the fact that an intracluster proton transfer reaction occurs when there are more than four water molecules within the cluster, leading to the formation of protonated water clusters and a phenyl radical, as per eq 1:

$$\{(C_6H_6) + (H_2O)_{n\geq 4}\} \rightarrow \{(C_6H_5^{\bullet}) + (H_2O)_{n\geq 4}H^+\} \quad (\text{for } n \geq 4) \quad (1)$$

In conjunction with the studies of the benzene cation, the interaction between the toluene cation and polar molecules is also of great interest. Due to the additional methyl group, the conjugated base of the toluene cation is a neutral benzyl radical with a stable π-system (Scheme 1). Brutschy and Bernstein have investigated the ion fragmentation and chemistry of toluene−water cluster ions by using resonance-enhanced two photon ionization (R2PI) spectroscopy and mass resolved excitation spectroscopy (MRES), respectively.[5,7] Their observations indicate that the proton begins to be extracted from the toluene cation when solvated by more than three water molecules, again indicating that there is a minimal number of solvating water molecules required for the proton transfer reaction to take place. Daly et al. have studied the clusters of toluene cation solvated by methanol molecules using high pressure mass spectrometry.[18] Their experiments show that two methanol molecules are necessary for the deprotonation of the toluene cation and the formation of the protonated methanol dimer. Observations of proton transfer reactions in these cluster systems can be rationalized by the proton affinity of the solvating clusters (Table 1).[19,20] The intracluster proton transfer reactions are highly size-

SCHEME 1

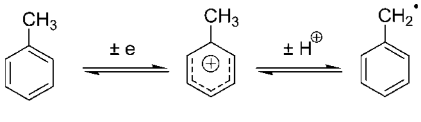

---

* To whom correspondence should be addressed. E-mail: garvey@buffalo.edu.

[†] Department of Chemistry, University at Buffalo, State University of New York at Buffalo.

[‡] Center for Computational Research, University at Buffalo, State University of New York at Buffalo.

10.1021/jp8041186 CCC: $40.75

TABLE 1: Proton Affinities of Selected Species

species	proton affinity[a] (kcal/mol)	species	proton affinity[b] (kcal/mol)
benzene	179	H_2O	167
phenyl	211	$(H_2O)_2$	195
toluene	187	$(H_2O)_3$	206
benzyl	198	$(H_2O)_4$	215
		$(H_2O)_5$	216
		CH_3OH	182
		$(CH_3OH)_2$	211
		$(CH_3OH)_3$	224
		$(CH_3OH)_4$	231
		$(CH_3OH)_5$	234

[a] Ref 19. [b] Ref 20.

dependent due to the proton affinity of the solvent molecules and a minimal number of solvent molecules are needed in order to extract the proton from the aromatic cation. This can only occur when the proton affinity of the solvent cluster exceeds that of the aromatic cation.

Although the critical cluster size to initiate the proton transfer has been investigated, it was also found in the studies of other benzene or toluene cations in medium sized $(H_2O)_n$ ($n \approx 25$) clusters, that the direct proton transfer reactions were not observed for larger clusters but instead a neutral radical-OH adduct with a protonated water subcluster was created.[21] This implies that the proton transfer reaction is highly dependent on the particular cluster structure at a certain cluster size. To the best of our knowledge, no investigation has been reported where such reactions have been studied as a function of cluster size to attempt to identify the changes that occur in different reaction channels. Previously, clusters of toluene and methanol, $\{(C_6H_5CH_3)(CH_3OH)_n\}^+$, have been studied but were limited to $n = 1$ and 2.[18] To explore larger clusters and find the critical size needed to turn off the proton transfer reaction, this present study probed the chemical reactivity of $\{(C_6H_5CH_3)(CH_3OH)_n\}^+$ cluster ions in a size range of $n = 1-7$.

$(C_6H_5CH_3)(CH_3OH)_n$ clusters first were formed in a continuous molecular beam source and then were ionized by electron impact ionization. The distribution of these ions was determined from the conventional mass spectrum while collision induced dissociation (CID) and metastable decay of mass-selected cluster ions were performed to characterize the preferred reaction channels, and to elucidate the structure of these clusters. Density functional theory (DFT) at the B3LYP/6−311+G* level was used to calculate the optimal geometry of clusters and to evaluate their relative energies. The reaction profiles were calculated based on the reaction coordinates of reactant and product clusters to understand the reaction energy barriers.

II. Experimental Section

The molecular beam apparatus employed for these experiments has been described elsewhere.[22] In brief, the toluene−methanol mixture was introduced by passing helium through a bubbler containing the liquid toluene and methanol reagents in a ratio of 1:2 by volume. The mixed vapor at a stagnation pressure of 1.5 atm was supersonically expanded through a 250-μm nozzle at a nozzle temperature of 291 K using a Campargue-type continuous molecular beam source.[23] The temperature of a neutral cluster is estimated to be approximately in the range of 40−100 K[24] due to the rapid cooling process achieved by the supersonic expansion. The neutral cluster beam was collimated by two conical nickel skimmers before entering the triple quadrupole mass spectrometer. A small fraction of the neutral clusters were ionized via electron impact ionization with an electron energy of 65.0 eV and an emission current of 3.0 mA. The estimated internal temperature of a cluster ion is in the range of 300−1000 K.[25] It was found that variation of the electron energy tended to either increase or decrease the ion intensities without any major shifts in the relative distribution of the various peaks.[26] Collinear ion optics are then used to focus and guide the ionized clusters into the triple quadrupole assembly (Extrel C-50). Both the first and third quadrupoles have a nominal mass range of 1200 amu and can be operated in either "rf" or "dc" mode. The second quadrupole is always in "rf-only" mode to guide the cluster ions to the third quadrupole and contains a gas collision cell for CID experiments. A conventional mass scan mode was produced by setting the first and the second quadrupoles to "rf-only" mode, and scanning the third quadrupole (Q3). For metastable decay and CID experiments, MS/MS spectra were obtained by mass-selecting the desired cluster ion with (Q1) and mass-analyzing the product ions with the third quadrupole mass filter. The mass resolution of the instrument is sufficient to characterize the ions of interest which differ by 1 amu. A laboratory frame collision energy of 10 eV is used, which is determined by the difference in the effective source potential and the dc level of the second quadrupole. For fixed laboratory frame collision energy, the relative collision energies (center-of-mass collision energy) for the various ions decreases as the ion mass increases, ranging between 1.1 and 2.5 eV. Reagent grade toluene and methanol were obtained from Merck, methanol-d_4 was from Aldrich, helium (>99.9%) and argon (>99.9%) were from Irish Welding Supply.

III. Theoretical Calculations

Optimal geometries of clusters were calculated at the DFT level of theory using the B3LYP[27,28] hybrid functional and utilizing the 6−311+G* basis set[29] (triple-ζ valence quality with diffuse and polarization functions) without any constraints, and allowing C_1 symmetry for all calculated cluster systems. The cluster bonding energy was calculated as an energy difference between the calculated energy of the cluster, and the sum of the calculated energies of the separated monomers. The zero-point vibrational energy is included in the calculated energies. A basis-set superposition-error correction was not employed in our calculations due to the high quality of the basis set used in our calculations.[30] This level of theory gives the cluster energy with the accuracy in a range between 1−3 kcal/mol. The reaction profiles were calculated with full geometry optimization of the cluster, for a fixed value of the reaction coordinate. Then the reaction coordinate was incrementally changed, and the calculation of the optimal geometry was repeated. The reaction coordinate was chosen as a difference between two interatomic distances, namely the distance between the aliphatic-hydrogen and carbon atoms of toluene, and the distance between the aliphatic-hydrogen atom of toluene and the oxygen atom of methanol. The calculations were performed using the Q-Chem program.[31]

IV. Results and Discussion

1. Mass Spectrum of $\{(C_6H_5CH_3)(CH_3OH)_n\}^+$ Cluster Ions. The mass spectrum for toluene−methanol heterocluster ions is shown in Figure 1. Only singly charged clusters were observed in this spectrum, hence, the *m*/*z* of each cluster will be referred to as its mass (in amu). This spectrum is dominated by the peaks of the toluene cation ($C_6H_5CH_3^+$, $m/z = 92$), tropylium ion ($C_7H_7^+$, $m/z = 91$) and the protonated methanol

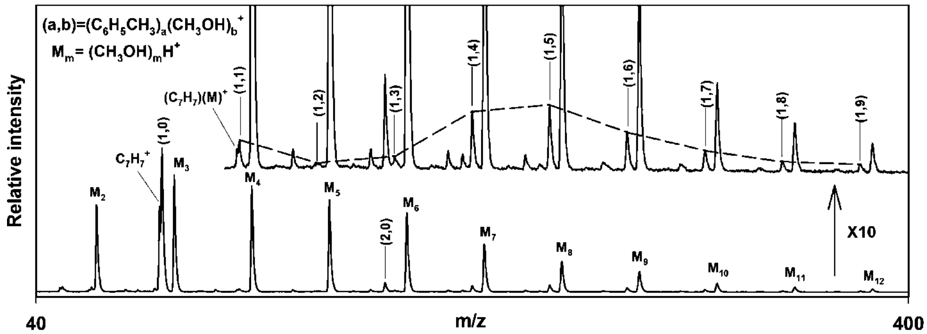

Figure 1. Survey mass spectrum of cluster ions formed in a toluene/methanol/helium expansion. The upper spectrum has been magnified 10×.

series $(CH_3OH)_mH^+$. Protonated methanol clusters are common product ions due to the exothermic proton transfer reactions within neat ionized methanol clusters as indicated by the following reaction channels:

$$(CH_3OH)_{m+1} + e^- \rightarrow \{(CH_3OH)_m + CH_3OH^{+\bullet}\} + 2e^- \quad \text{Ionization} \quad (2a)$$

$$\{(CH_3OH)_m + CH_3OH^{+\bullet}\} \rightarrow (CH_3OH)_mH^+ + CH_3O^\bullet \quad \text{(Proton Transfer)} \quad (2b)$$

Upon expanding the intensity 10×, the series of $\{(C_6H_5CH_3)(CH_3OH)_{1-9}\}^+$ clusters ions can now be observed. Generation of this type of cluster can be expressed as follows:

$$(C_6H_5CH_3)(CH_3OH)_{n+m} + e^- \rightarrow \{(C_6H_5CH_3)(CH_3OH)_{n+m}\}^+ + 2e^- \quad \text{Ionization} \quad (3a)$$

$$\{(C_6H_5CH_3)(CH_3OH)_{n+m}\}^+ \rightarrow \{(C_6H_5CH_3)(CH_3OH)_n\}^+ + mCH_3OH \quad \text{Evaporation} \quad (3b)$$

The relative ion intensity of this series of cluster ions is indicated by the connecting dashed line. Cluster series composed of different combinations are also seen in the mass spectrum but only those clusters of interest are assigned in this work. Note that in the present study, the $(CH_3OH)_3H^+$ cluster ion is the most abundant peak in the series of protonated methanol cluster ions and the $\{(C_6H_5CH_3)(CH_3OH)_5\}^+$ cluster ion is the most intense peak in its series. The most intense peak in each series often indicates a cluster ion with a uniquely stable structure or a global minimum where further monomer evaporation or reaction is not favorable and is referred to as the magic number cluster size.

2. CID Mass Spectra of $\{(C_6H_5CH_3)(CH_3OH)_n\}^+$ Cluster Ions, $n = 1-7$. CID analysis has been proven to be an extremely powerful technique to elucidate the structures of parent ions and also to study chemical reactions within mass-selected cluster ions.[22,32] Cluster ions of interest are first mass-selected by the first quadrupole and then guided through the second quadrupole containing a collision cell. In the present study, argon was used as the collision gas, and the collision cell pressure was maintained at (9.0 ± 1.0) × 10^{-4} torr during the CID experiments. The background pressure in the mass spectrometer chamber was approximately (4.0 ± 1.0) × 10^{-6} torr with the beam on and collision gas in the collision chamber, and (2.0 ± 1.0) × 10^{-7} torr with no beam on and no collision gas in the collision cell.

After undergoing inelastic collisions with argon, the cluster ions become vibrationally activated and can then undergo monomer evaporation or even chemical reactions within the cluster. Given the experimental conditions, each selected ion was intended to experience multiple collisions with argon to produce an extensive fragmentation pattern. The reaction product ions exiting the collision cell are finally mass-analyzed by the third quadrupole. In Figure 2, each CID spectrum in the same series of clusters is superimposed and offset in order to easily visualize and compare the various reaction channels and fragments as a function as increasing cluster size.

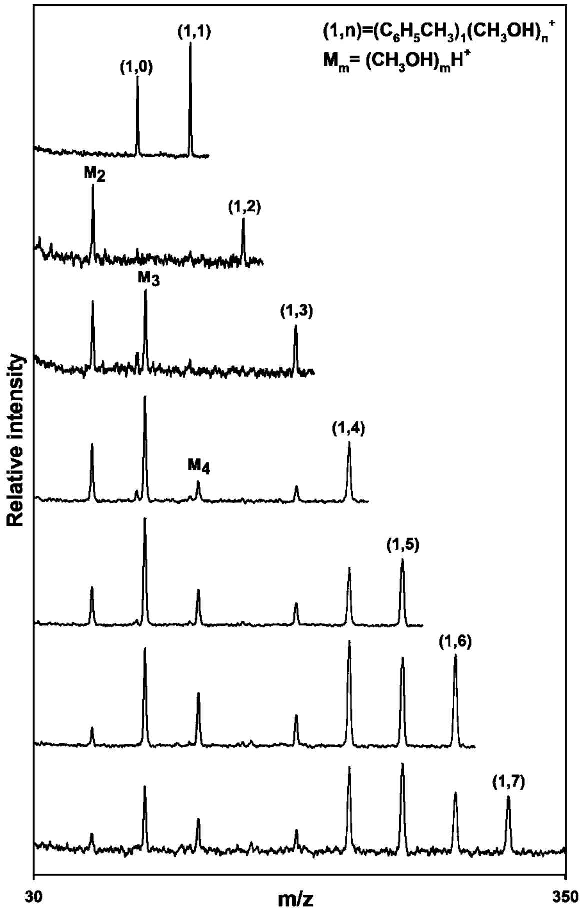

Figure 2. CID mass spectra of $(C_6H_5CH_3)_1(CH_3OH)_n^+$, $n = 1-7$. M_n denotes protonated methanol clusters and $(1,n)$ denotes clusters of type of $(C_6H_5CH_3)_1(CH_3OH)_n^+$.

For $n = 1$, the only observed channel is the evaporative loss of a neutral methanol molecule:

$$\{(C_6H_5CH_3)(CH_3OH)\}^+ \xrightarrow{\text{CID}} C_6H_5CH_3^+ + CH_3OH \quad (4)$$

This observation is explained by the fact that the proton affinity of methanol {PA = 182 kcal/mol} is not sufficient to

SCHEME 2

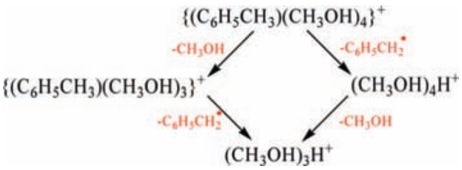

compete with that of the benzyl radical {PA = 198 kcal/mol} for possession of the proton.[19,20,33] However, this also indicates that the positive charge within the cluster is mainly retained on the toluene moiety due to the substantially lower ionization potential (8.83 eV) of toluene compared to that of methanol (10.84 eV).[30]

For $n = 2-4$, two channels are observed ($n \geq m$):

$$\{(C_6H_5CH_3)(CH_3OH)_n\}^+$$

$$\xrightarrow{\text{CID}} \{(C_6H_5CH_3)(CH_3OH)_{n\text{-}m}\}^+ + mCH_3OH \tag{5a}$$

$$\xrightarrow{\text{CID}} (CH_3OH)_{n-m}H^+ + mCH_3OH + C_6H_5CH_2^{\bullet} \tag{5b}$$

Reaction 5a represents the sequential evaporative loss of neutral methanol molecules from the toluene−methanol cluster ions, while reaction 5b is the proton transfer reaction from the toluene cation to methanol clusters to form a protonated methanol cluster and a benzyl radical. Reaction 5b is the main process observed for $n = 2$ and $n = 3$ where the direct proton transfer reaction occurs between the toluene cation and the methanol subclusters (i.e., $M_n = (CH_3OH)_nH^+$). We note that this is consistent with the observation that the intracluster proton transfer reactions are size-dependent based on the proton affinity of the solvent molecules (Table 1). However, for $n = 4$ the direct proton transfer to form M_4 is not the preferred reaction channel but rather M_3 is the preferred reaction product. Therefore, two possible reaction channels (Scheme 2) may occur and both can lead to the formation of M_3. Subsequently, this M_3 product can then form M_2 by evaporative loss of a methanol.

For $n = 5-7$, the CID spectra of these three cluster ions illustrate a very consistent pattern indicating that no direct proton transfer occurs within the cluster ions. According to Table 1, the proton affinity of methanol clusters increases as a function of increasing cluster size, indicating that larger methanol clusters are expected to have a stronger ability to extract the proton. However, we observe that the mass-selected parent ions have to evaporate methanol monomers down to a certain size of 4 before the proton transfer is observed. Any "direct" proton transfer reaction from toluene to the methanol subcluster does not occur preferentially for $n \geq 5$. We have considered the possibility that the proton does transfer directly from toluene to the methanol subcluster for $n \geq 5$ and is followed by the evaporative loss of methanols. Such a sequence is at most a very minor reaction channel since no relative daughter ions were observed, such as the formation of M_5 and M_6 for $n = 7$.

To confirm the observed result above, the isotopically labeled CD_3OD was mixed with $C_6H_5CH_3$ in order to determine the source in the proton transfer (see Supporting Information Figure S1). The isotopic spectra show that for $n \geq 4$, there is a very minor reaction pathway for the proton transfer within the methanol subcluster to form deuterated methanol cluster ions; however, the dominant peaks in the spectra are protonated ions, indicating that the dominant proton source is the toluene. This is consistent with the observation above and hence validates such size-restricted proton transfer reactions within the toluene−methanol cluster ions.

TABLE 2: Metastable Decay Channels for $(C_6H_5CH_3)(CH_3OH)_n{}^+$Cluster Ions[a]

n	−M	−B	−B and −M	−2M	− B and −2M
1	0	0			
2	0	0	0	0	
3	0	82.4	17.6	0	0
4	11.7	35.3	47.1	0	5.9
5	40	0	20	10	30
6	70	0	0	30	0
7	70	0	0	30	0

[a] Daughter ion intensities as a percentage of the total daughter ion signal observed in the metastable decay mass spectra for the series $(C_6H_5CH_3)(CH_3OH)_n{}^+$, where the observed decay channels are CH_3OH (M) and $C_6H_5CH_2^{\bullet}$ (B). The pressure in the collision cell ranged from 1.5×10^{-6} to 2.5×10^{-6} torr.

3. Metastable Decay Mass Spectra. Metastable decay was performed in order to make a qualitative comparison with CID experiments for the decomposition processes of individual cluster ions of the series $\{(C_6H_5CH_3)(CH_3OH)_{n=1-7}\}^+$. The results are summarized in Table 2, where the fragment ions are normalized to the percentage of all observed product ions. The experimental conditions under which the metastable decay mass spectra were acquired are identical to those employed for the CID mass spectra given above except with no collision gas in the collision cell. The pressure within the cell was $(1.5 \pm 1.0) \times 10^{-6}$ Torr for all metastable experiments. The parent ion of interest was mass-selected in the first quadrupole and then passed into the evacuated collision cell with a laboratory frame ion energy of 10 eV. The metastable decay spectra were quite simple and straightforward to interpret. In the case of $n = 1$ and 2, there was no unimolecular decomposition channel observed in their metastable decay mass spectra, suggesting a strong interaction between the toluene cation and the methanol monomers. However, there were five decomposition channels for the series of $\{(C_6H_5CH_3)(CH_3OH)_{n=3-7}\}^+$: loss of CH_3OH, loss of $C_6H_5CH_2^{\bullet}$, loss of $C_6H_5CH_2^{\bullet} + CH_3OH$, loss of 2 CH_3OH, and loss of $C_6H_5CH_2^{\bullet} + 2\ CH_3OH$. We note that the simple loss of $C_6H_5CH_2^{\bullet}$ is observed only for $n = 3$ and $n = 4$ which is again direct evidence for the proton transfer reaction within these clusters. For $n = 5$, the simultaneous loss of both benzyl and methanol was observed. Such results suggest that a secondary channel for simultaneous loss of benzyl radical and methanol may exist but there was no product ion observed for direct proton transfer. If a direct proton transfer preferentially takes place within these large clusters and is followed by the loss of a neutral methanol, then the formation of protonated methanol clusters is expected to be observed. However, there is no direct proton transfer observed for $n > 5$ and the only metastable decay channel is the loss of CH_3OH.

4. Optimized Structures of $\{(C_6H_5CH_3)(CH_3OH)_{n=1-4}\}^+$ Cluster Ions. Figure 4 displays the optimized structures for the $\{(C_6H_5CH_3)(CH_3OH)_n\}^+$ clusters. Many stable isomeric structures were found for each size of cluster and they were categorized based on the optimized structures of the first methanol added to the toluene cation. For $n = 2-4$, focus in the present work is on the cooperative effect of the methanol subcluster due to the hydrogen bonds.

$\{(C_6H_5CH_3)(CH_3OH)_1\}^+$. Two isomers were calculated for the $n = 1$ cluster by placing the "solvent" methanol either adjacent to the methyl group, at the opposite side of the methyl group or on the top of the aromatic ring, as shown in Figure 3(a). The isomer with the lowest energy is 1-I where the oxygen

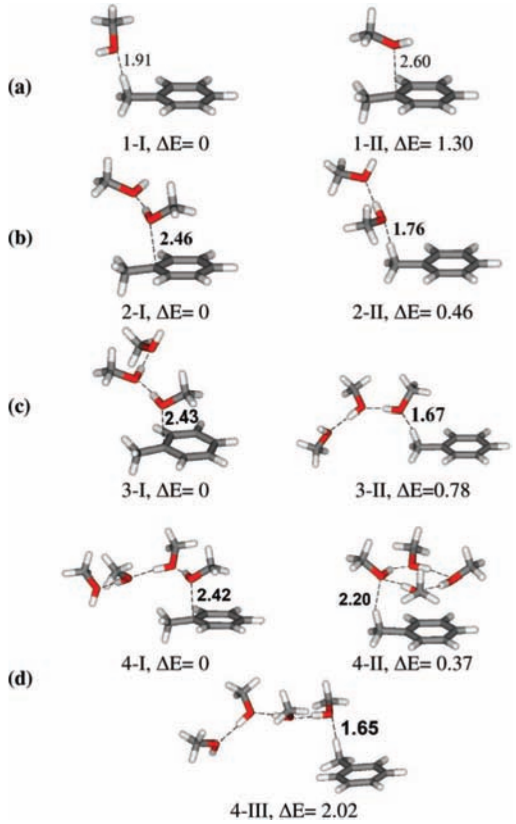

Figure 3. Optimized structures of $\{(C_6H_5CH_3)(CH_3OH)_{n=1-4}\}^+$ cluster ions at the B3LYP/6−311+G* level. Bond lengths are expressed in Angstroms, Å. *E* is the energy, in kcal/mol, relative to the most stable isomer.

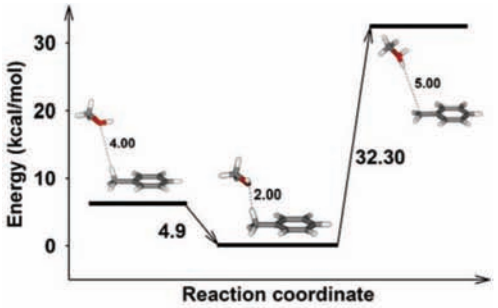

(a) $\{(C_6H_5CH_3)(CH_3OH)\}^+ \rightarrow (CH_3OH)H^+ + C_6H_5CH_2^{\bullet}$

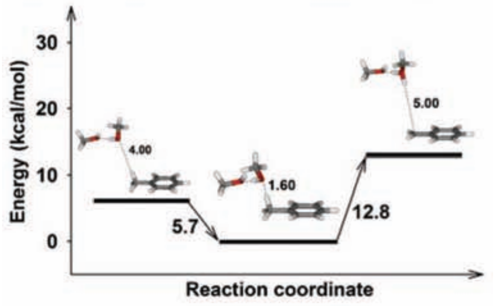

(b) $\{(C_6H_5CH_3)(CH_3OH)_2\}^+ \rightarrow (CH_3OH)_2H^+ + C_6H_5CH_2^{\bullet}$

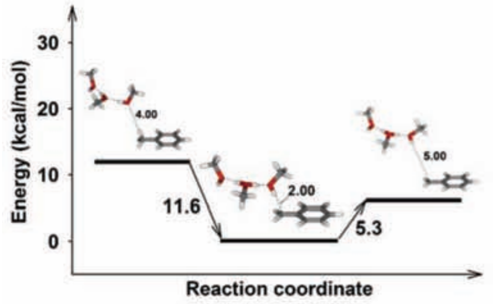

(c) $\{(C_6H_5CH_3)(CH_3OH)_3\}^+ \rightarrow (CH_3OH)_3H^+ + C_6H_5CH_2^{\bullet}$

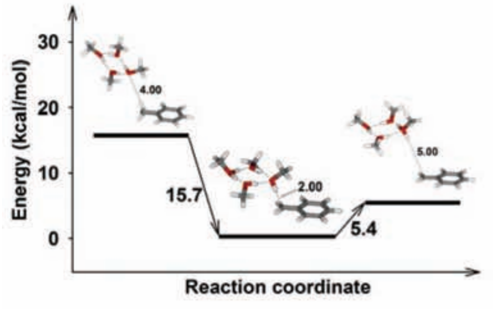

(d) $\{(C_6H_5CH_3)(CH_3OH)_4\}^+ \rightarrow (CH_3OH)_4H^+ + C_6H_5CH_2^{\bullet}$

Figure 4. Reaction coordinate based energy profiles for $\{(C_6H_5CH_3)(CH_3OH)_n\}^+ \rightarrow (C_6H_5CH_2^{\bullet})(CH_3OH)_nH^+$, $n = 1-4$. Bond lengths are expressed in Angstroms. The numbers above the arrows are the energy difference (kcal/mol) between the structures at the two reaction coordinates.

of the methanol is hydrogen-bonded to the aliphatic-hydrogen atom of the toluene. The "on ring" structure of isomer 1-II reflects the interaction between the methanol moiety and the aromatic ring of the toluene cation where partial charge transfer is expected to occur to recover the electron density deficiency of the aromatic ring. We calculated the charge distribution between the toluene moiety and the methanol moiety based on the *Mulliken Net Atomic Charge* from the optimized structure calculation for each cluster isomer. As indicated in Table 3, for Isomer 1-II approximately 20% of the electron density is shifted to the toluene cation in this structure.

$\{(C_6H_5CH_3)(CH_3OH)_2\}^+$. For $n = 2$, two isomers were calculated by placing an additional methanol adjacent to the optimized structures of $n = 1$.The lowest energy isomer is isomer 2-I, where two methanols are bonded together via a conventional hydrogen bond and located on the aromatic ring of the toluene cation. With the additional methanol, electron density is transferred to the toluene cation[22] such that the toluene moiety only retains approximately 62% of the positive charge (Table 3). For isomer 2-II, the cooperative effect of the methanol subcluster enhances the strength of the hydrogen bond by reducing the bond distance to 1.76 Å, which is comparable to a conventional neutral hydrogen bond of 1.80 Å.[34] As seen in Figure 2, we observe the direct proton transfer reaction at $n = 2$ and isomer 2-II might be considered as the prototypical geometry for the reaction to take place, however it is not the isomer with the lowest energy.

$\{(C_6H_5CH_3)(CH_3OH)_3\}^+$. The lowest energy structure (Isomer 3-I) for $n = 3$ is obtained by adding a methanol to the isomer 2-I to form another hydrogen bond within the methanol subcluster such that two hydrogen bonds connect three methanols in a chain structure and interact with the aromatic ring through the methanol oxygen. Approximately 44% of the electron density is transferred to the toluene cation, indicating that the additional methanol is pulling more electron density toward the interactive oxygen. However, the C...O distance does not decrease much, indicating a repulsion between the methyl groups of the toluene cation and the methanol molecules, and between the lone pair electrons of oxygen and the π-electrons. For isomer 3-II, the additional methanol substantially decreases the hydrogen bond distance to 1.67 Å. Such a structure is expected as the initial structure for the proton transfer reaction to occur but again is not the lowest energy structure from the calculation.

TABLE 3: Charge Distribution within Isomers

isomer	toluene moiety	methanol moiety
1-I	0.92	0.08
1-II	0.80	0.20
2-I	0.62	0.38
2-II	0.81	0.19
3-I	0.56	0.44
3-II	0.74	0.26
4-I	0.55	0.45
4-II	0.63	0.37
4-III	0.72	0.28

$\{(C_6H_5CH_3)(CH_3OH)_4\}^+$. For $n = 4$, isomer 4-I has the C...O distance reduced to 2.42 Å and approximately 45% of the electron density is transferred from the methanol moiety to the toluene moiety. This result is essentially identical with the isomer 3-I but with an additional methanol, suggesting that the fourth methanol does not necessarily pull more electron density toward the interacting oxygen when forming a third hydrogen bond. Isomer 4-II is only 0.37 kcal/mol higher than the isomer 4-I, indicating that the methanol subcluster also is able to form a cyclic structure when $n \geq 4$. The hydrogen bond length of the isomer 4-III is 1.65 Å which is only 0.02 Å shorter than that of the isomer 3-II, similar to the comparison between the isomer 3-I and 4-I. This result indicates that the fourth methanol does not contribute much in either type of cluster structure.

In summary, the optimized structures of $\{(C_6H_5CH_3)(CH_3OH)_{n=1-4}\}^+$ cluster ions indicate that there are two cluster structures, the "on ring" and "on methyl group" structures. Additions of up to three methanols to either of these two sites of the toluene moiety gradually enhance either interaction.[22] However, this cooperative effect does not occur when the fourth methanol is added, implying that the additions of fifth, sixth, and seventh methanol might also have as little effect as the fourth one (see optimized cluster structures for $n = 5-7$ in Supporting Information Figure S2). The formation of such ringed structures make the clusters more stable, especially for $n = 4-6$ as shown in Figure 1.

5. Reaction Profiles of $\{(C_6H_5CH_3)(CH_3OH)_n\}^+ \rightarrow (C_6H_5CH_2^{\bullet})(CH_3OH)_n H^+$, $n = 1-4$. Figure 4 shows reaction profiles for $n = 1-4$. The left structures represent the toluene and methanol moieties separated by 4 Å. They are otherwise fully geometrically optimized calculations, and the reaction coordinate was incrementally changed in the reaction profile calculations. The middle structures are the minimal energy structures during the reaction and the right structures are the protonated methanols and benzyl radical separated by 5 Å. For $n = 1$, the lowest energy structure has a 2.00 Å $-H_2CH\cdots O$ distance when the proton is still on the toluene cation and the energy cost is 32.3 kcal/mol for the lowest energy structure to form protonated methanol and the benzyl radical separated by 5Å. According to Table 1, the proton transferred structure is expected to be the lowest energy structure when two methanols are present, however for $n = 2$ as shown in Figure 4(b), the proton resides on the toluene cation for the lowest energy structure. The $-H_2CH\cdots O$ distance is reduced to 1.60 Å with the additional methanol and the energy required to form the protonated methanol dimer and benzyl radical has been drastically reduced to 12.8 kcal/mol by the additional methanol. In the $n = 3$ reaction profile, the proton is transferred to the methanol subcluster for the lowest energy structure, indicating that the addition of a third methanol allows the intracluster proton transfer reaction to occur without any energy barrier. The energy required for the dissociation of the protonated methanol trimer and a benzyl radical is ~5.3 kcal/mol. For $n = 4$, the ring structure methanol subcluster was chosen as the starting geometry, and it was found that the proton is also transferred to the methanol subcluster in the lowest energy structure. However, the energy for the dissociation of protonated methanol tetramer and benzyl radical requires ~5.4 kcal/mol which is about the same as the dissociation of the protonated methanol trimer and the benzyl radical for $n = 3$. The fourth methanol enables the methanol subcluster to form a ring structure which would seem to geometrically favor the proton transfer, but this structure does not reduce the energy required for the dissociation.

SCHEME 3

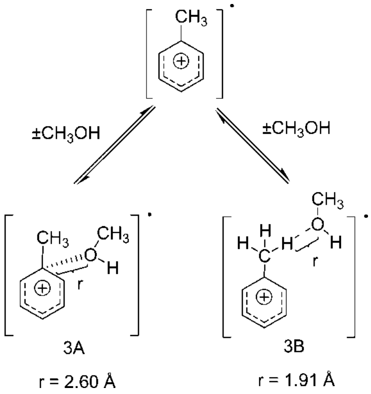

V. Discussion

The present work shows that for $\{(C_6H_5CH_3)(CH_3OH)_n\}^+$ cluster ions size-restricted proton transfer reaction within clusters can be observed via tandem mass spectrometry. From the calculational results, methanol exhibits two types of behavior with the toluene cation (Scheme 3). In the first interaction type, shown in the 3A structure, the methanol subcluster interacts with the electron deficient aromatic ring and there is a net transfer of electron density from the methanol subcluster to the toluene cation. In the second interaction type, shown in 3B, an unconventional H-bond forms with a methyl group hydrogen and there is less electron density transfer. The distance between interactive atoms compresses and electron density transfer increases as up to three methanols are added. This is caused by a cooperative effect of the methanols forming a subcluster where more electron density is pulled toward the interacting oxygen as the number of methanols increases. There is little or no advantage either for structural stabilization or to promote the proton transfer reaction when the fourth methanol is added. For $n \geq 5$, these larger clusters have to lose the methanol monomers down to at least $n = 4$ in order to extract the proton but $(CH_3OH)_3H^+$ remains the most preferred reaction product. As the number of methanols increases, the possibility of forming methanol ring structures makes larger clusters more stable but is not favorable for the "direct" proton transfer reaction. Therefore, sequential loss of methanol monomers is the necessary transition to break the ring structure prior to the proton transfer reaction. The neat protonated methanol cluster, $(CH_3OH)_3H^+$ is the "magic number" structure that has an enhanced stability because it represents the first complete solvation shell of the $(CH_3OH)H^+$ ion[35] The qualitative discussions above suggest that $n = 3$ plays a very important role not only for neat methanol cluster but also for heterocluster ions.

According to Table 1, the methanol dimer subcluster should be able to extract the proton from the methyl group but the reaction profile in Figure S6 of the Supporting Information shows that the proton is still bonded to the toluene carbon. This result indicates that for $n = 2$ the 3A structure (Scheme 3) is significant since the proton affinity and the restoration of the ring aromaticity in the benzyl radical product should both tend to drive the proton transfer reaction. In the CID experiment, we observed the direct proton transfer reaction and dissociation for $n = 2$, indicating that collision with argon activates this cluster chemistry. The CID experiment for $n = 3$ also shows the direct proton transfer reaction product and its corresponding reaction profile suggests that the intracluster proton transfer reaction is energetically favorable within cluster structures. The third methanol is the driving force to allow the reaction since it increases the gross proton affinity of the methanol subcluster to counter the interaction within the cluster. As indicated by the CID result for $n = 4$, the direct proton transfer reaction is not as efficient as that for $n = 3$, which is consistent with the calculational result that the addition of a fourth methanol does not contribute further stabilization for either the cluster structure or the final product.

VI. Conclusions

To summarize, the present work supports 5 general conclusions: (1) The collision induced dissociated proton transfer reaction within the toluene−methanol cluster ions is size-restricted at $2 \leq n \leq 4$. For $n \geq 5$ clusters, methanol monomers must be evaporated off to at least $n = 4$ for this reaction to occur. (2) The metastable decay experiments confirm that the energetically favored reactions can lead to the formation of protonated methanol clusters (3) There are two types of toluene−methanol cluster structures that play important roles, an “on ring” structure where the methanol subcluster partially transfers electron density to stabilize the electron deficiency of the toluene cation, and an “on methyl group” structure where the methanol subcluster forms a H-bond with a methyl group hydrogen. The former one is more stable then the later one if $2 \leq n \leq 4$. However, the “on methyl group” site has the proper configuration for the proton transfer. (4) Optimized structures of $\{(C_6H_5CH_3)(CH_3OH)_n\}^+$ show that the addition of the fourth methanol provides little or no additional stabilization of the cluster structures. (5) The reaction profiles were consistent with the metastable decay and CID experiments in that the preferred reaction product of $(CH_3OH)_3H^+$ is driven by both the proton affinity and the enhanced stability of forming this product.

Acknowledgment. T.R.F. gratefully acknowledges support of NIH SBIR Grant No. 2R44GM065617-02. This work was performed in part at SUNY-Buffalo’s Center for Computational Research.

Supporting Information Available: Figure S1 shows the CID mass spectra of $(C_6H_5CH_3)_1(CD_3OD)_n{}^+$, $n = 1-7$. Figure S2 shows the optimized structures of $\{(C_6H_5CH_3)(CH_3OH)_{n=5-7}\}^+$ cluster ions. This information is available free of charge via the Internet at http://pubs.acs.org.

References and Notes

(1) Vöhringer-Martinez, E.; Hansmann, B.; Hernandez, H.; Francisco, J. S.; Troe, J.; Abel, B. *Science* **2007**, *315*, 497.

(2) Castleman, A. W., Jr. *Clusters of Atoms and Molecules II*; Haberland, H., Ed.; Springer-Verlag: Berlin, 1994; Chapter 2.4.

(3) *Ion and Cluster Ion Spectroscopy and Structure*; Maier, J. P., Ed.; Elsevier: Amsterdam, 1989.

(4) Meot-Ner (Mautner) , M. *Chem. Rev* **2005**, *105*, 213.

(5) Bernstein, E. R. *J. Phys. Chem.* **1992**, *96*, 10105.

(6) Brutschy, B. *Chem. Rev.* **2000**, *100*, 3891.

(7) Brutschy, B. *Chem. Rev.* **1992**, *92*, 1567.

(8) Ibrahim, Y.; Alsharaeh, E.; Dias, K.; Meot-Ner (Mautner) , M.; El-Shall, M. S. *J. Am. Chem. Soc.* **2004**, *126*, 12766.

(9) Ibrahim, Y. M.; Meot-Ner (Mautner) , M.; Alsharaeh, E. H.; El-Shall, M. S.; Scheiner, S. *J. Am. Chem. Soc.* **2005**, *127*, 7053.

(10) Miyazaki, M.; Fujii, A.; Ebata, T.; Mikami, N. *Chem. Phys. Lett.* **2001**, *349*, 431.

(11) Miyazaki, M.; Fujii, A.; Ebata, T.; Mikami, N. *Phys. Chem. Chem. Phys.* **2003**, *5*, 1137.

(12) Miyazaki, M.; Fujii, A.; Ebata, T.; Mikami, N. *J. Phys. Chem. A* **2004**, *108*, 8269.

(13) Enomoto, S.; Miyazaki, M.; Fujii, A.; Mikami, N. *J. Phys. Chem. A* **2005**, *109*, 9471.

(14) Li, S.; Bernstein, E. R. *J. Chem. Phys.* **1992**, *97*, 792.

(15) Nicholas, M.; Boyd, R. J.; Arnold, D. R. *Can. J. Chem.* **1982**, *60*, 3011.

(16) Sehested, K.; Holcman, J. *J. Phys. Chem.* **1978**, *82*, 651.

(17) Eberhardt, M. K. *J. Am. Chem. Soc.* **1981**, *103*, 3876.

(18) Daly, G. M.; Meot-Ner, M.; Pithawalla, Y. B.; El-Shall, M. S. *J. Chem. Phys.* **1996**, *104*, 796.

(19) Hunter, E. P.; Lias, S. G. *J. Phys. Chem. Ref. Data* **1998**, *27* (3), 413.

(20) Knochenmuss, R.; Cheshnovsky, O.; Leutwyler, S. *Chem. Phys. Lett.* **1988**, *144*, 317.

(21) Courty, A.; Mons, M.; LeCalvé, J.; Piuzzi, F.; Dimicoli, I. *J. Phys. Chem. A* **1997**, *101*, 1445.

(22) Chiang, C.-T.; Freindorf, M.; Furlani, T.; DeLeon, R. L.; Richard, J. P.; Garvey, J. F. *J. Phys. Chem. A* **2007**, *111*, 6068.

(23) Campargue, R. J. *Phys. Chem.* **1984**, *88*, 4466.

(24) Dong, F.; Heinbuch, S.; Rocca, J. J.; Bernstein, E. R. *J. Chem. Phys.* **2006**, *124*, 224319.

(25) McLuckey, S. A.; Glish, G. L.; Asano, K. G. *Int. J. Mass Spectrom. Ion Proc.* **1991**, *109*, 171.

(26) Garvey, J. F.; Herron, W. J.; Vaidyanathan, G. *Chem. Rev.* **1994**, *94*, 1999.

(27) Garvey, J. F.; Herron, W. J.; Vaidyanathan, G. *Chem. Rev.* **1994**, *94*, 1999. (a) Becke, A. D. *Phys. Rev. A* **1988**, *38*, 3098.

(28) Lee, C.; Yang, W.; Parr, R. G. *Phys. Rev. B* **1988**, *37*, 785.

(29) Hehre, W. J.; Radom L.; Schleyer, P.v.R.; Pople, J. A. *Ab Initio Molecular Orbital Theory*; Wiley: New York, 1986.

(30) Rablen, P. R.; Lockman, J. W.; Jorgensen, W. L. *J. Phys. Chem. A* **1998**, *102*, 3782.

(31) Kong, J.; White, C. A.; Krylov, A. I.; Sherrill, C. D.; Adamson, R. D.; Furlani, T. R.; Lee, M. S.; Lee, A. M.; Gwaltney, S. R.; Adams, T. R.; Ochsenfeld, C.; Gilbert, A. T. B.; Kedziora, G. S.; Rassolov, V. A.; Maurice, D. R.; Nair, N.; Shao, Y.; Besley, N. A.; Maslen, P. E.; Dombroski, J. P.; Dachsel, H.; Zhang, W. M.; Korambath, P. P.; Baker, J.; Byrd, E. F. C.; Van Voorhis, T.; Oumi, M.; Hirata, S.; Hsu, C. P.; Ishikawa, N.; Florian, J.; Warshel, A.; Johnson, B. G.; Gill, P. M. W.; Head-Gordon, M.; Pople, J. A. *J. Comput. Chem.* **2000**, *21*, 1532.

(32) Lyktey, M. M. Y.; DeLeon, R. L.; Shores, K. S.; Furlani, T. R.; Garvey, J. F. *J. Phys. Chem. A* **2000**, *104*, 5197.

(33) *CRC Handbook of Chemistry and Physics*, 76th ed.; Lide, D. R., Ed.; CRC Press: Boca Raton, FL, 1995.

(34) Zumdahl, S. S. *Chemistry*, 3rd ed.; D. C. Heath and Co.: MA, 1993.

(35) Grimsrud, E. P.; Kebarle, P. *J. Am. Chem. Soc.* **1973**, *95*, 7939.

JP8041186